

# Haematite pseudomicrofossils present in the 3.5-billion-year-old Apex Chert

Craig P. Marshall, Julienne R. Emry and Alison Olcott Marshall\*

**Microstructures in the ~3.5 Gyr Apex Chert Formation were initially described as the oldest bacterial fossils on Earth over 20 years ago<sup>1</sup>. However, the identification of the structures (which resemble cyanobacteria) as biological in origin remains controversial<sup>1–13</sup>. Here we determine the petrology and geochemistry of similar structures from the original Apex Chert locality using thin sections and Raman spectroscopy. Based on the microscopic examination of thin sections, we identify features similar to those previously identified as microfossils as a series of quartz and haematite-filled fractures. Raman spectroscopy of the fractures shows that carbonaceous material is not, as previously reported, associated with the structures, but is instead disseminated in the surrounding quartz matrix. We suggest that although the microstructures analysed are not microfossils, the presence of carbonaceous material in the surrounding matrix is consistent with the existence of microbial life at this time, and with evidence of early Archaean life<sup>14,15</sup> found at other sites. Furthermore, we caution against identifying microstructures as biological in origin without a full morphological and geochemical assessment.**

The Apex Chert, in the Warrawoona Group in Western Australia<sup>1</sup>, has been described to contain fossilized filamentous cyanobacteria<sup>1</sup>, fossils that have been formally described and named<sup>9</sup>. These proposed fossils, described from palaeontological thin sections about 300  $\mu\text{m}$  thick, were reported only in rounded fossiliferous clasts embedded in a siliceous matrix, interpreted to be deposited in a shallow marine setting<sup>1,9</sup>. Furthermore, some microfossils were described as iron-stained<sup>9</sup>. For almost a decade, these microfossils were widely accepted by the scientific community<sup>16</sup>, until the origin of the structures, as well as their geological context, was reinterpreted<sup>2</sup>. Remapping the outcrops led to the interpretation that the rocks were formed in a hydrothermal setting<sup>2–5,17</sup>. Further study of the original thin sections and newly collected specimens exhibited filamentous branching microstructures inconsistent with biology<sup>2–5</sup>. Moreover, structures similar to the previously described microfossils were discovered in lone clasts as well as in multiple generations of the fabric<sup>2–5</sup>. Although the palaeoenvironmental reinterpretation was accepted<sup>13</sup>, the branching was dismissed as artefacts of the automontaging software used to create the photomicrographs<sup>10</sup>. Furthermore, both studies used Raman spectroscopy to investigate the Apex Chert microstructures. Although both concluded that the opaque structures were composed of carbonaceous material<sup>2,12</sup>, they disagreed in the interpretation of this material. Whereas one interpreted the data as indicating abiotic amorphous graphite<sup>2</sup>, the other took the data as proof that the structures were composed of biogenic kerogen<sup>12</sup>. Although carbonaceous material has since been found in isolated Apex Chert samples using synchrotron radiation-based spectroscopy (STXM; ref. 6), there is still no scientific consensus on whether the filamentous microstructures are biogenic.

New samples were collected from the original fossil locality during the Geological Survey of Western Australia's (GSWA) field trip to the Pilbara Craton<sup>17</sup>. We performed petrographic analyses of this material in 30  $\mu\text{m}$ -thick petrographic sections (thin sections) and 300  $\mu\text{m}$ -thick palaeontological sections (thick sections) prepared from the same blank, which yield markedly different perspectives of the same material. Both thin and thick sections contain features similar to the clasts described previously<sup>9</sup> (Fig. 1a,b). Within the thick sections, in clast-like features (Fig. 1a) and dispersed through the matrix (Fig. 1b), as well as within cross-cutting veins (Supplementary Fig. S1), are features similar to the previously described microfossils (Fig. 1c–f). These opaque microstructures are reddish-to-dark-brown (Fig. 1a), often sinuous (Fig. 1f) and segmented, appearing septate (Fig. 1c–e), and have a similar diameter to the putative microfossils<sup>9</sup> (Fig. 1h). However, in the corresponding thin sections, these structures appear as fractures intermittently filled with a light mineral and dark microplaty mineral (Fig. 1g, Supplementary Figs S2, S3). In thin section, the light material has a coarse block-like texture, with crystal sizes ranging from 4  $\mu\text{m}$  to 65  $\mu\text{m}$ , with an average size of 17.3  $\mu\text{m}$ , in contrast to the matrix, which is microcrystalline, with crystal sizes ranging from 0.3  $\mu\text{m}$  to 6  $\mu\text{m}$ , with an average size of 2.2  $\mu\text{m}$  (Supplementary Fig. S2). This difference is lost in the thick sections, where all of the material surrounding the microstructures seems to be amorphous chert (Fig. 1c–f).

Raman spectroscopy was used to identify the fracture-fill material on the thin and thick sections. The representative spectra acquired from the dark material in the thin and thick sections show diagnostic vibrational modes at 225 and 498  $\text{cm}^{-1}$  ( $A_{1g}$  symmetry modes), and 247, 293, 299, 412, and 613  $\text{cm}^{-1}$  ( $E_g$  symmetry modes) indicative of haematite<sup>18</sup> (Fig. 2a, Supplementary Figs S2, S3). The additional intense broad band at 1,320  $\text{cm}^{-1}$  is also indicative of haematite, assigned to an overtone of a forbidden odd symmetry infrared-active phonon at about 660  $\text{cm}^{-1}$ , probably activated by disorder<sup>19</sup>. The representative spectra acquired from the clear material in the thick and thin sections show diagnostic vibrational modes at 206, 464, and 511  $\text{cm}^{-1}$  ( $A_1$  symmetry modes), consistent with quartz<sup>20</sup> (Fig. 2b, Supplementary Figs S2, S3). In contrast, the matrix in which the fractures are found has quartz bands at 206, 464, and 511  $\text{cm}^{-1}$  ( $A_1$  symmetry modes), but also two broad bands at 1,350 and 1,600  $\text{cm}^{-1}$ , assigned to  $A_{1g}$  and  $E_{2g}$  symmetry modes of disordered carbonaceous materials (Fig. 2c). These bands, colloquially referred to as the 'D' and 'G' bands, respectively, are indicative of the presence of disseminated carbonaceous material<sup>21</sup>.

The identification of the opaque mineral as haematite is in contrast to previously published interpretations of Raman spectroscopic data, both point-spectra and 3D images, concluding that the putative microfossils are composed of carbonaceous material<sup>2,5,11–13</sup>. As the specimen types were not analysed, it is

Department of Geology, University of Kansas, Lawrence Kansas, 66045, USA. \*e-mail: olcott@ku.edu.

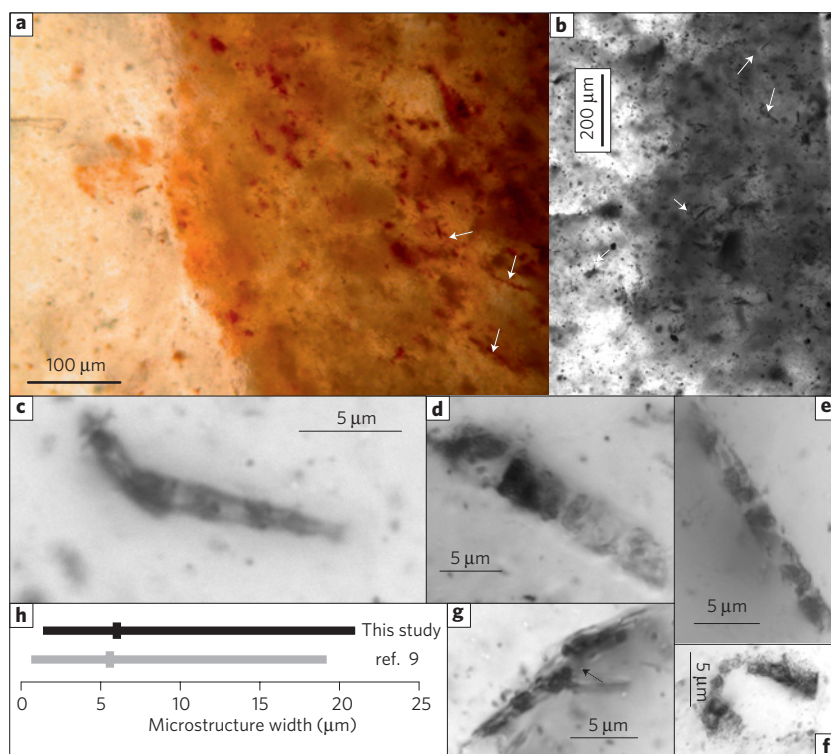


**Figure 1 | Photomicrographs showing features similar to those previously described, and a graph comparing the size of each. a**, Feature similar to previously described clasts<sup>9</sup> (arrows indicate microstructures). **b**, Clast-like feature with microstructures (indicated by arrows) inside and outside the clast, as previously reported<sup>2</sup>. **c–f**, Opaque microstructures in thick section appear septated, similar to previously described microfossils<sup>9</sup>. Note that the microstructure in **c** has both an opaque outer wall and septa-like features, with large clear patches inside, similar to Fig. 1g in ref. 12 (*P. conicoterminatum*). In contrast, **d–f** have large opaque patches separated by clear septate-like structures, similar to Fig. 1f in ref. 12 (*P. delicatulum*). **g**, Similar microstructure in thin section, showing microplaty opaque mineral within a clear vein (arrow). **h**, Average size range of the microstructures described here compared to putative microfossils<sup>9</sup> ( $n = 50$ , standard deviation = 3.9).

possible that there is just a morphological similarity between the microstructures described here and previously described *bona fide* microfossils found in the same locality. However, as the microstructures most morphologically similar to the previously described microfossils contained only haematite and quartz (Supplementary Figs S4–S7), we feel instead that the disparity between our Raman spectra and previously published data can best be explained in three ways. First, the reddish-brown colour of the microstructures was thought to indicate that they were composed of organic carbon of moderate thermal maturity<sup>2,12</sup>, although the line-shape of the carbon bands in the previously published Raman spectra are characteristic of highly thermally mature, and thus black, organic carbon<sup>22</sup>. Second, point-spectrum Raman spectroscopy is a surface technique, and under the experimental conditions used here and in previous point-spectral studies<sup>2,5,12</sup> the laser penetrates less than 1 µm into a siliceous sample<sup>23</sup>. Thus, if an opaque microstructure is more than 1 µm below the surface, the resulting Raman point-spectrum will in fact be of the overlying matrix. As the Apex Chert matrix is optically clear, features that seem to be surficial can in reality be embedded deep within a thick section. Given the similarity between the Raman spectra of the matrix, which our analyses have revealed contains finely disseminated carbonaceous material, and the previously reported Raman spectra of the microstructures<sup>2,12</sup> (Fig. 2d) it seems likely that the previous point-spectra Raman analyses indicating carbonaceous material in the microstructures were Raman spectra of the overlying matrix.

Finally, although 3D Raman images of the putative microfossils were said to demonstrate their carbonaceous composition<sup>11,13,24</sup>, it seems likely that the wide haematite band at 1,320 cm<sup>-1</sup> was misinterpreted as the D band at 1,350 cm<sup>-1</sup>. In contrast to

point-spectra analyses, 3D Raman spectroscopy is said to be able to penetrate over 65 µm into thick sections<sup>24</sup>, thus eliminating the problem of analysing the matrix rather than the structure of interest. This technique has been used to create 3D images of the microstructures found in the Apex Chert<sup>11,13,24</sup>. To do this, a depth series of Raman scans across the same X,Y plane are collected and stacked. However, unlike point-spectra Raman analyses, where individual spectra are presented, in 2D and 3D Raman imaging the intensity of the major band found in all of the spectra is used to generate an image of the microstructure<sup>24</sup>. Thus, the resulting data generate an image that does not show the presence of individual Raman bands. Previous work presented 3D Raman images created from the most intense band found in scans of the carbon first-order region (800–1,800 cm<sup>-1</sup>; refs 11,13,24). However, even if the opaque material does not have the bands indicative of carbonaceous material (Fig. 2a), a 3D Raman image of a segmented microstructure (Fig. 3b) constructed on the band intensity at 1,350 cm<sup>-1</sup>, the D band, would still produce an image, because of the presence of the broad haematite band at 1,320 cm<sup>-1</sup> (Fig. 3c,d). Furthermore, it is possible to misidentify the haematite band at 1,320 cm<sup>-1</sup> as a carbon vibrational mode at 1,350 cm<sup>-1</sup> (ref. 25), especially if the associated haematite vibrational modes found in the ‘mineral-fingerprint region’ (100–700 cm<sup>-1</sup>) are not included in the scanned range (Fig. 3a). Thus, based on the broad band at 1,320 cm<sup>-1</sup> produced by the haematite-filled fractures (Fig. 2a), it seems possible that the previously published 3D Raman images<sup>11,13,24</sup> show the distribution of haematite and quartz, not carbonaceous material and quartz (Fig. 3c,d).

More recent chemical analyses using STXM have been interpreted as showing that the microstructures are carbonaceous<sup>6</sup>.

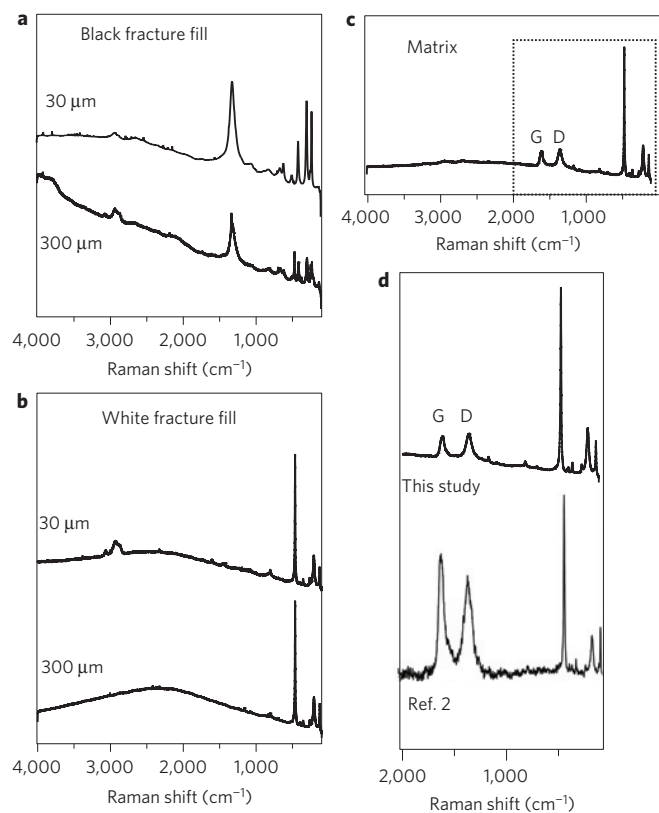


**Figure 2 | Raman spectra collected from vein-fill minerals, the matrix, and a comparison between the matrix and a previously published Raman spectrum.** **a**, Spectra from the black fracture fill reveal haematite, **b** spectra from the white fracture fill reveal quartz. **c**, The spectrum of the matrix reveals quartz and carbonaceous material, marked with 'G' and 'D'. Box indicates area in **d**, comparing the matrix spectrum to a previously published spectrum claimed to be of microstructures<sup>2</sup> (reproduced with permission). The two spectra are almost identical; the differences between the D and G bands are due to artefacts introduced by their baseline correction<sup>2,21</sup>, and thus their relative intensities cannot be compared to the intensity of the quartz bands. These cannot be directly compared to the spectra in ref. 12, as the latter were of the carbon first-order region (800–1,800  $\text{cm}^{-1}$ ).

However, these analyses were performed on mechanically separated and microtomed chert pieces, thus it is not possible to link the carbonaceous material with a particular microstructural feature of the chert. In contrast, our *in situ* Raman spectroscopic measurements demonstrate that the carbonaceous material is found in association with the matrix, not with the opaque microstructures.

Although the Apex Chert microstructures have many of the widely accepted characteristics of *bona fide* fossil microbes, these structures do not seem to be biogenic, nor do they resemble iron-stained or iron-replaced microfossils. Previously, it has been argued that a microstructure that is (1) cylindrical, (2) with a limited range of widths, (3) uniform diameter through its length, (4) some sinuosity relative to its width and length, and, (5) if permineralized, hollow in the centre, is definitively biogenic<sup>26</sup>. However, there is nothing specifically biogenic about the second, third and fourth criteria, as mineral veins are known to have the same characteristics<sup>27</sup>. The fifth criterion is an important one for biogenicity, as 3D Raman spectroscopic images of younger microfossils<sup>11</sup> have shown distinctive hollow interiors. Similarly, studies of microbial filaments replaced or stained by iron precipitates all demonstrate that this type of preservation results in a sheath of iron minerals surrounding a hollow centre<sup>28,29</sup>. Although

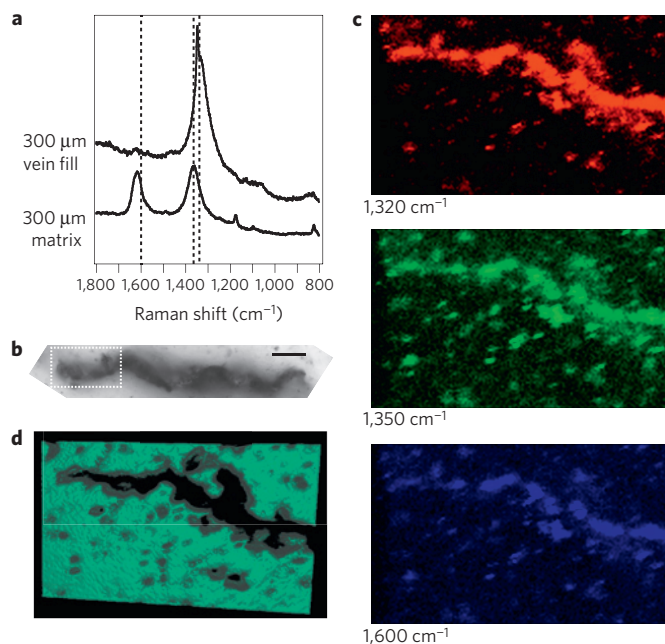


**Figure 3 | Raman spectra and images demonstrating how the haematite band at 1,320  $\text{cm}^{-1}$  can lead to the appearance of carbonaceous material.**

**a**, Spectra of the opaque vein-fill and the matrix indicating the proximity of the haematite band at 1,320  $\text{cm}^{-1}$  and the D band at 1,350  $\text{cm}^{-1}$ . **b**, Photomicrograph of microstructure analysed in **c** and **d**. Note the similarity to the putative microfossil illustrated in Fig. 4b in ref. 9 ('*P. amoenum*'). **c**, 2D images of the intensity at the indicated Raman shifts. The image of the G band (1,600  $\text{cm}^{-1}$ ) does not recreate the structure visible in **b**, whereas the D band (1,350  $\text{cm}^{-1}$ ) does, despite the lack of carbon (**a**). The image of the haematite band intensity at 1,320  $\text{cm}^{-1}$  replicates the microstructure. **d**, 3D image of **b**, green is quartz. Note the patches in middle of the microstructure.

it has been claimed that the Apex Chert microfossils are hollow in the centre<sup>11</sup> 3D Raman spectroscopic images indicate that they are actually solid material containing a few isolated patches of quartz (Fig. 3d, see Fig. 4p in ref. 11). This morphology is more similar to that seen in veins filled with haematite and quartz, which can have the appearance of septated filaments<sup>26</sup>, than to that seen in septated filamentous microfossils<sup>11</sup>. Furthermore, given the fact that the matrix, not the microstructures, contains carbonaceous material, which, by definition, is recalcitrant and difficult to remobilize<sup>21,22</sup>, it is improbable that a carbonaceous microfossil could be entirely replaced with haematite while the surrounding carbonaceous matrix remains unaltered. Finally, these microstructures are found both within the original matrix and within later cross-cutting features (Supplementary Fig. S1), whereas *bona fide* microfossils should be found only within the original matrix<sup>26</sup>.

The likely identification of these microstructures as fractures filled with haematite indicates that care must be taken when searching for ancient traces of microbial life. Morphology alone can be misleading and open to interpretation, which may explain why no microfossils have been identified in other samples of the Apex Chert<sup>8</sup> or in the slides of the original material now housed at the GSWA (ref. 30). Although chemical analyses can be powerful tools in the search for ancient life, they, too, must be applied judiciously, as chemical data can also mislead. However, although the previously described Apex Chert microbiota may be pseudofossils, there is still a growing body of evidence from other localities<sup>14,15</sup> indicative of microbial life in the early Archaean. Furthermore, our data revealed carbonaceous material disseminated throughout the matrix, carbonaceous material previously described as having

a molecular structure similar to known biogenic carbonaceous material<sup>6</sup>, thus the Apex Chert could still contain evidence of life on early Earth, albeit in a form that is not so easily recognizable.

## Methods

Petrographic analyses of the Apex Chert were conducted on standard 30  $\mu\text{m}$ -thick petrographic sections and 300  $\mu\text{m}$ -thick palaeontological sections. Optical microscopy was performed with an Olympus BX51 System Microscope, and the width of a randomized selection of 50 microstructures and the size of a randomized selection of crystals was measured at  $\times 50$  using the calibrated measurement SPOT software. Raman spectra were collected on standard 30  $\mu\text{m}$ -thick petrographic sections and 300  $\mu\text{m}$ -thick palaeontological sections produced by Burnham Petrographics. The Raman spectra were acquired on a Renishaw inVia Reflex Raman Microprobe with a Peltier-cooled charge-coupled device detector. The collection optics is based on a Leica DM LM microscope. A refractive glass  $\times 50$  objective lens was used to focus the laser on a 2- $\mu\text{m}$  spot and collect the backscattered radiation. The 514.5 nm line of a 5 watt Ar<sup>+</sup> laser (Stabilite 2017 laser; Spectra-Physics) oriented normal to the sample was used to excite the sample. The instrument was calibrated against the Raman signal of Si at 520  $\text{cm}^{-1}$  using a silicon wafer (111). A surface laser power of 1.0–1.5 mW was used to minimize laser-induced heating of the samples. For Raman point-spectra, an accumulation time of 30 s and ten scans were used, which gave an adequate signal-to-noise ratio for the spectra. The scan ranges were collected either over the full range 100–4,000  $\text{cm}^{-1}$  or over the carbon first-order region 800–1,800  $\text{cm}^{-1}$ . Raman images were made by collecting Streamline images with an accumulation time of 0.1 s and scans from 400 to 1,700  $\text{cm}^{-1}$  every 0.2  $\mu\text{m}$  down into the thick section from 0.2  $\mu\text{m}$  to 4.6  $\mu\text{m}$ . These images were then stitched together in ImageJ and ImageVis3D.

Received 14 June 2010; accepted 14 January 2011; published online 20 February 2011

## References

- Schopf, J. W. & Packer, B. M. Early Archean (3.3-billion to 3.5-billion-year-old) microfossils from Warrawoona Group, Australia. *Science* **237**, 70–73 (1987).
- Brasier, M. D. *et al.* Questioning the evidence for Earth's oldest fossils. *Nature* **416**, 76–81 (2002).
- Brasier, M. D., Green, O. R., Lindsay, J. F. & Steele, A. Earth's oldest (3.5 Gyr) fossils and the 'Early Eden' hypothesis: Questioning the evidence. *Origins Life Evol. B* **34**, 257–269 (2004).
- Brasier, M. D., McLoughlin, N., Green, O. R. & Wacey, D. A fresh look at the fossil evidence for early Archean cellular life. *Phil. Trans. R. Soc. B* **361**, 887–902 (2006).
- Brasier, M. D. *et al.* Critical testing of Earth's oldest putative fossil assemblage from the  $\sim 3.5$  Gyr Apex chert, Chinaman Creek, Western Australia. *Precamb. Res.* **140**, 55–102 (2005).
- De Gregorio, B. T., Sharp, T. G., Flynn, G. J., Wirick, S. & Hervig, R. L. Biogenic origin for Earth's oldest putative microfossils. *Geology* **37**, 631–634 (2009).
- Pasteris, J. D. & Wopenka, B. Necessary, but not sufficient: Raman identification of disordered carbon as a signature of ancient life. *Astrobiology* **3**, 727–738 (2003).
- Pinti, D. L., Mineau, R. & Clement, V. Hydrothermal alteration and microfossil artefacts of the 3,465-million-year-old Apex chert. *Nature Geosci.* **2**, 640–643 (2009).
- Schopf, J. W. Microfossils of the early Archean Apex Chert: New evidence of the antiquity of life. *Science* **260**, 640–646 (1993).
- Schopf, J. W. in *The Precambrian Earth: Tempos and Events (Developments in Precambrian Geology 12)* (eds Eriksson, P. G., Altermann, W., Nelson, D. R., Mueller, W. U. & Cateneanu, O.) 516–539 (Elsevier, 2004).
- Schopf, J. W. & Kudryavtsev, A. B. Confocal laser scanning microscopy and Raman imagery of ancient microscopic fossils. *Precamb. Res.* **173**, 39–49 (2009).
- Schopf, J. W., Kudryavtsev, A. B., Agresti, D. G., Wdowiak, T. J. & Czaja, A. D. Laser-Raman imagery of Earth's earliest fossils. *Nature* **416**, 73–76 (2002).
- Schopf, J. W., Kudryavtsev, A. B., Czaja, A. D. & Tripathi, A. B. Evidence of Archean life: Stromatolites and microfossils. *Precamb. Res.* **158**, 141–155 (2007).
- Walsh, M. M. & Lowe, D. R. Filamentous microfossils from the 3,500-Myr-old Onverwacht Group, Barberton Mountain Land, South Africa. *Nature* **314**, 530–532 (1985).
- Walsh, M. M. Microfossils and possible microfossils from the Early Archean Onverwacht Group, Barberton Mountain Land, South Africa. *Precamb. Res.* **54**, 271–293 (1992).
- Knoll, A. H. & Walter, M. W. The limits of palaeontological knowledge: Finding the gold among the dross. *Ciba Found. Symp.* **202**, 198–209 (1996).
- Van Kranendonk, M. L. & Pirajno, F. Geochemistry of metabasalts and hydrothermal alteration zones associated with c. 3.45 Gyr chert and barite deposits: Implications for the geological setting of the Warrawoona Group, Pilbara Craton, Australia. *Geochem. Explorat. Environ. Anal.* **4**, 253–278 (2004).
- de Faria, D. L. A., Silva, S. V. & de Oliveira, M. T. Raman microspectroscopy of some iron oxides and oxyhydroxides. *J. Raman Spectrosc.* **28**, 873–878 (1997).
- Wang, L., Zhu, J., Yan, Y., Xie, Y. & Wang, C. Micro-structural characterization of red decorations of red and green colour porcelain. *J. Raman Spectrosc.* **40**, 998–1003 (2004).
- Kingma, K. J. & Hemley, R. J. Raman spectroscopic study of microcrystalline silica. *Am. Mineral.* **79**, 269–273 (1994).
- Marshall, C. P., Edwards, H. G. M. & Jehlicka, J. Understanding the application of Raman spectroscopy to the detection of traces of life. *Astrobiology* **10**, 229–243 (2010).
- Pasteris, J. D. & Wopenka, B. Raman spectra of graphite as indicators of degree of metamorphism. *Can. Mineral.* **29**, 1–9 (1991).
- Yan, J. Laser micro-Raman spectroscopy of single-point diamond machined silicon substrates. *J. Appl. Phys.* **95**, 2094–2101 (2004).
- Schopf, J. W. & Kudryavtsev, A. B. Three-dimensional Raman imagery of Precambrian microscopic organisms. *Geobiology* **3**, 1–12 (2005).
- Toporski, J., Fries, M., Steele, A., Nittler, L. & Kress, M. Sweeping the skies: Stardust and the origin of our Solar System. *GIT Imaging Microsc.* **4**, 38–40 (2004).
- Schopf, J. W., Kudryavtsev, A. B., Sugitani, K. & Walter, M. W. Precambrian microbe-like pseudofossils: A promising solution to the problem. *Precamb. Res.* **179**, 191–205 (2010).
- Nicholson, R. & Ejiófor, I. B. The three-dimensional morphology of arrays of echelon and sigmoidal, mineral-filled fractures: Data from north Cornwall. *J. Geol. Soc.* **144**, 79–83 (1987).
- Boyd, T. D. & Scott, S. D. Microbial and hydrothermal aspects of ferric oxyhydroxides and ferrosic hydroxides: The example of Franklin Seamount, Western Woodlark Basin, Papua New Guinea. *Geochem. Trans.* **2**, 45–56 (2001).
- Parenteau, M. N. & Cady, S. L. Microbial biosignatures in iron-mineralized phototrophic mats at Chocolate Pots Hot Springs, Yellowstone National Park, United States. *Palaio* **25**, 97–111 (2010).
- Dalton, R. Microfossils: Squaring up over ancient life. *Nature* **417**, 782–784 (2002).

## Acknowledgements

Thanks to Australian Research Council for funding, M. Walter and M. Van Kranendonk for field assistance and helpful discussions, R. Goldstein for paragenesis advice, and A. Walton for access to his colour photomicrography facility.

## Author contributions

C.P.M. collected the samples, J.R.E. collected the Raman data, A.O.M. and J.R.E. collected the photomicrographs, C.P.M. and A.O.M. interpreted the data, and A.O.M. wrote the paper with contributions from C.P.M.

## Additional information

The authors declare no competing financial interests. Supplementary information accompanies this paper on [www.nature.com/naturegeoscience](http://www.nature.com/naturegeoscience). Reprints and permissions information is available online at <http://npg.nature.com/reprintsandpermissions>. Correspondence and requests for materials should be addressed to A.O.M.